



CERN-EP-2018-116
9 May 2018

Suppression of $\Lambda(1520)$ resonance production in central Pb–Pb collisions at $\sqrt{s_{NN}} = 2.76$ TeV

ALICE Collaboration *

Abstract

The production yield of the $\Lambda(1520)$ baryon resonance is measured at mid-rapidity in Pb–Pb collisions at $\sqrt{s_{NN}} = 2.76$ TeV with the ALICE detector at the LHC. The measurement is performed in the $\Lambda(1520) \rightarrow pK^-$ (and charge conjugate) hadronic decay channel as a function of the transverse momentum (p_T) and collision centrality. The p_T -integrated production rate of $\Lambda(1520)$ relative to Λ in central collisions is suppressed by about a factor of 2 with respect to peripheral collisions. This is the first observation of the suppression of a baryonic resonance at LHC and the first evidence of $\Lambda(1520)$ suppression in heavy-ion collisions. The measured $\Lambda(1520)/\Lambda$ ratio in central collisions is smaller than the value predicted by the statistical hadronisation model calculations. The shape of the measured p_T distribution and the centrality dependence of the suppression are reproduced by the EPOS3 Monte Carlo event generator. The measurement adds further support to the formation of a dense hadronic phase in the final stages of the evolution of the fireball created in heavy-ion collisions, lasting long enough to cause a significant reduction in the observable yield of short-lived resonances.

© 2018 CERN for the benefit of the ALICE Collaboration.

Reproduction of this article or parts of it is allowed as specified in the CC-BY-4.0 license.

*See Appendix A for the list of collaboration members

High-energy heavy-ion collisions provide an excellent means to study the properties of nuclear matter under extreme conditions and the phase transition to a deconfined state of quarks and gluons (Quark-Gluon Plasma, QGP [1]) predicted by lattice QCD calculations [2]. The bulk properties of the matter created in high-energy nuclear reactions have been widely studied at the Relativistic Heavy Ion Collider (RHIC) and at the Large Hadron Collider (LHC), and are well described by hydrodynamic and statistical models. The initial hot and dense partonic matter rapidly expands and cools, eventually undergoing a transition from the QGP to a hadron gas phase [3]. The relative abundances of stable particles are consistent with chemical equilibrium and are successfully described by Statistical Hadronisation Models (SHMs) [4–6]. They are determined by the “chemical freeze-out” temperature T_{ch} and the baryochemical potential μ_{B} [4, 7], reflecting the thermodynamic characteristics of the so-called “chemical freeze-out”. In the final stage of the collision a dense hadron gas is expected to form and to expand until the system eventually decouples when elastic interactions cease. Hadronic resonances with lifetimes shorter than or comparable to the timescale of the fireball evolution (a few fm/c) are sensitive probes of the dynamics and properties of the medium formed after hadronisation [8]. Within the SHM, they are expected to be produced with abundances consistent with the chemical equilibrium parameters T_{ch} and μ_{B} , but the measured yields might be modified after the chemical freeze-out by the hadronic phase. Due to their short lifetimes, resonances can decay within the hadronic medium, which can alter or destroy the correlation among the decay daughters via interactions (re-scattering) with the surrounding hadrons, hence reducing the observed yield. Alternatively, an increase (re-generation) might also be possible due to resonance formation in the hadronic phase [9]. The observed yield of hadronic resonances depends on the resonance lifetime, the duration of the hadronic phase and the relative scattering cross-section of the decay daughters within the hadronic medium.

Recent results from the ALICE Collaboration in Pb–Pb collisions at $\sqrt{s_{\text{NN}}} = 2.76$ TeV [10] show that the production yields of the $K^*(892)^0$ resonance are suppressed in central collisions with respect to peripheral collisions and are overestimated by SHM predictions. This phenomenon might be due to the short $K^*(892)^0$ lifetime ($\tau \sim 4$ fm/c) and suggests the dominance of destructive re-scattering over re-generation processes in the hadronic phase. No suppression is observed for the longer-lived $\phi(1020)$ meson ($\tau \sim 46$ fm/c), indicating that it decays mostly outside the fireball. Both observations are in agreement with the calculations of EPOS3, a model that includes a microscopic description of the hadronic phase [11]. Within this model, the lifetime of the hadronic phase formed in central Pb–Pb collisions at $\sqrt{s_{\text{NN}}} = 2.76$ TeV is predicted to be ~ 10 fm/c. The measurement of the production of the $\Lambda(1520)$ baryonic resonance, owing to its characteristic lifetime ($\tau \sim 12.6$ fm/c), serves as an excellent probe to further constrain the formation, the evolution and the characteristics of the hadronic phase.

In this Letter, we present the first measurement of $\Lambda(1520)$ production in Pb–Pb collisions at $\sqrt{s_{\text{NN}}} = 2.76$ TeV. The measurement is performed at midrapidity, $|y| < 0.5$, with the ALICE detector [12] at the LHC and is based on an analysis of about 15 million minimum-bias Pb–Pb collisions recorded in 2010. Previous results on $\Lambda(1520)$ production in high-energy hadronic collisions have been reported by STAR in pp, d–Au and Au–Au collisions at $\sqrt{s_{\text{NN}}} = 200$ GeV at RHIC [13, 14]. A detailed description of the ALICE experimental apparatus and its performance can be found in [15]. The relevant features of the main detectors utilised in this analysis are outlined here. The V0 detector is composed of two scintillator hodoscopes, placed on either side of the interaction point and covers the pseudorapidity regions $2.8 < \eta < 5.1$ and $-3.7 < \eta < -1.7$, respectively. It is employed for triggering, background suppression and collision-centrality determination. The Inner Tracking System (ITS) and the Time-Projection Chamber (TPC) provide vertex reconstruction and charged-particle tracking in the central barrel, within a solenoidal magnetic field of 0.5 T. The ITS is a high-resolution tracker made of six cylindrical layers of silicon detectors. The TPC is a large cylindrical drift detector of radial and longitudinal dimensions of about $85 < r < 247$ cm and $-250 < z < 250$ cm, respectively. Charged-hadron identification is performed by the TPC via specific ionisation energy-loss (dE/dx) and by the Time-Of-Flight (TOF) detector. The TOF is located at a radius of 370–399 cm and measures the particle time-of-flight with a resolution of

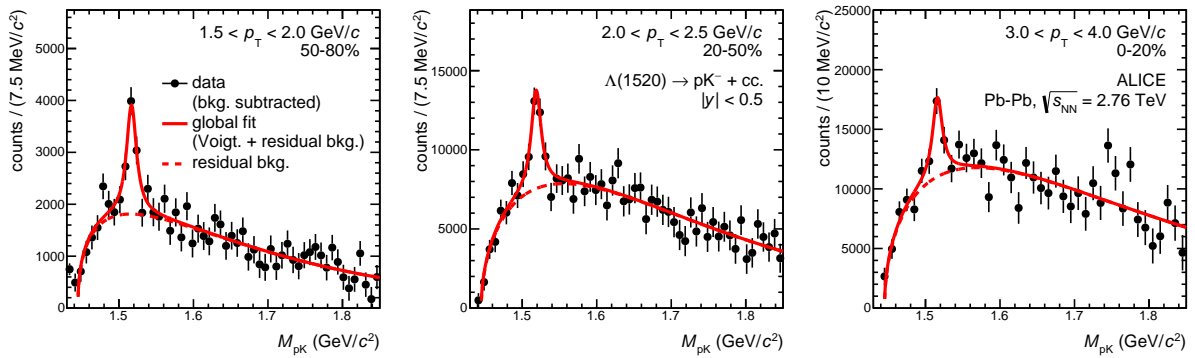


Fig. 1: Example invariant-mass distributions of the $\Lambda(1520) \rightarrow pK^-$ (and charged conjugate) reconstruction after subtraction of the mixed-event background. The solid line represents the global fit (signal + residual background) to the data while the dashed line indicates the estimated residual background. The error bars indicate the statistical uncertainties of the data.

about 80 ps, allowing hadron identification at higher momenta. A minimum-bias trigger was configured to select hadronic events with high efficiency, requiring a combination of hits in the two innermost layers of the ITS and in the V0 detector. The contamination from beam-induced background is removed offline, as discussed in detail in [16, 17]. The collision centrality is determined based on the signal amplitude of the V0 detector, whose response is proportional to the event multiplicity. A complete description of the event selection and centrality determination can be found in [18].

The $\Lambda(1520)$ resonance is reconstructed via invariant-mass analysis of its decay daughters in the hadronic decay channel $\Lambda(1520) \rightarrow pK^-$ (and charge conjugate, cc.), with a branching ratio of $22.5 \pm 0.5\%$ [19]. Particle and antiparticle states are combined to enhance the statistical significance of the reconstructed signal. $\Lambda(1520)$ refers to their sum in the following, unless otherwise specified. Candidate daughters are selected from tracks reconstructed by the ITS and TPC, are required to have $p_T > 150$ MeV/c and are restricted to the pseudorapidity range $|\eta| < 0.8$ for uniform acceptance and efficiency performance. Furthermore, a cut on the impact parameter to the primary vertex is applied to reduce contamination from secondary tracks emanating from weak decays or from interactions with the detector material. Details on the track selection can be found in [10]. Kaons and protons are identified from the combined information of the track dE/dx in the TPC and the time-of-flight measured by the TOF. The invariant-mass distribution of unlike-sign pairs of selected kaon and proton tracks is constructed for each centrality class and p_T interval. The rapidity of the candidate $\Lambda(1520)$ is required to be within $|y| < 0.5$. A large source of background from random combinations of uncorrelated pairs affects the invariant-mass spectrum. A mixed-event technique [20] is employed to estimate the combinatorial background, using unlike-sign proton and kaon tracks taken from different events with similar characteristics. The background is normalised and corrected for event-mixing distortions using a fit to the mixed/same-event ratio of like-sign pairs. Figure 1 shows examples of the reconstructed invariant-mass distribution after background subtraction. The $\Lambda(1520)$ raw yield is then extracted by means of a global fit, where a Voigtian function (the convolution of the non-relativistic Breit-Wigner with the Gaussian detector resolution) is used to describe the signal. The shape of the residual background resembles that of a Maxwell-Boltzmann distribution, therefore the residual background is fitted with a similar functional form

$$f_{\text{background}}(m_{pK}) = B \sqrt{(m_{pK} - m_{\text{cutoff}})^n C^{3/2}} \exp[-C(m_{pK} - m_{\text{cutoff}})^n],$$

where B (normalization), m_{cutoff} (low-mass cut-off), C and n are free parameters.

The raw yields are corrected for the decay branching fraction and for detector acceptance, reconstruction, track-selection and particle-identification efficiency, evaluated through a detailed Monte Carlo sim-

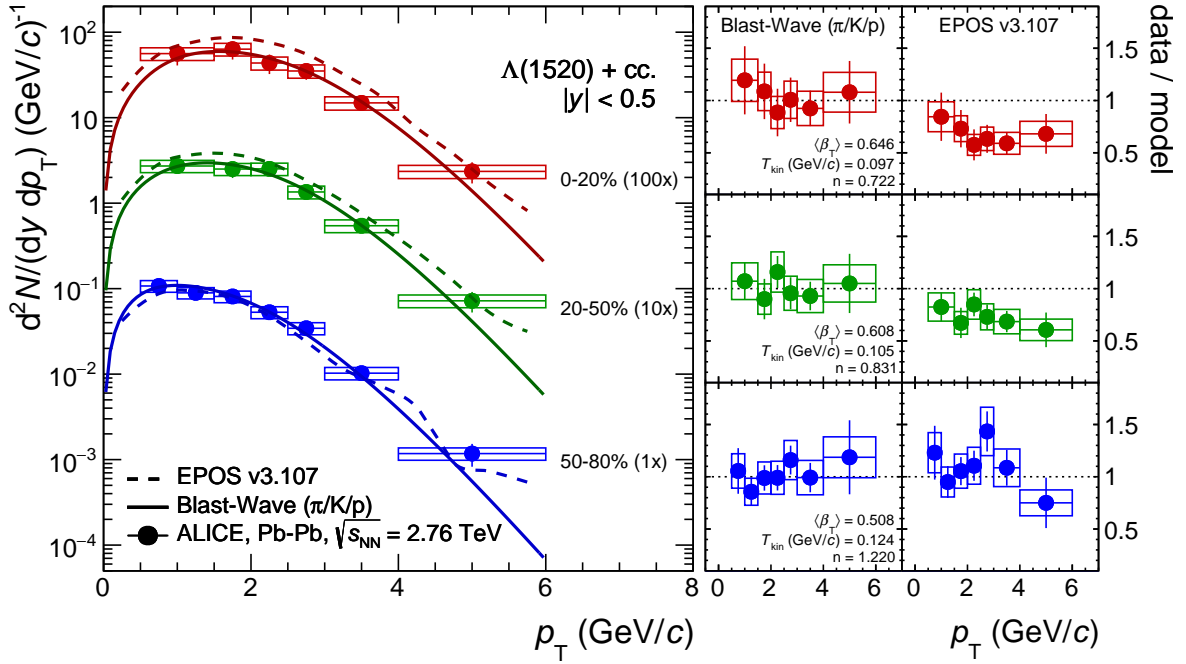


Fig. 2: (left) p_T -differential yields of $\Lambda(1520)$ at midrapidity, $|y| < 0.5$, in the centrality classes 0–20%, 20–50% and 50–80%. The solid and dashed curves represent predictions from the Blast-Wave model (normalisation fitted to the data) and EPOS3, respectively. (right) Ratio of the data to the Blast-Wave and EPOS3 predictions.

ulation of the ALICE detector. Simulation events are produced using the HIJING Monte Carlo event generator [21] with the addition of $\Lambda(1520)$ signals (particle and antiparticle states). Particle transport is performed by GEANT3 [22].

The main sources of systematic uncertainty on the corrected yields are summarised in Tab. 1. They include the signal extraction procedures as well as the contributions related to the efficiency corrections (true p_T distribution, track selection, particle identification, material budget and hadronic cross-section) and event normalisation. A significant fraction of this uncertainty, estimated to be about 12%, is common to all centrality classes.

	0–20%	20–50%	50–80%
Signal extraction	12	11	9
Global tracking efficiency	10 - 10.5	10 - 10.5	10 - 10.5
TOF matching efficiency	1 - 6.5	1 - 6.5	0 - 6.5
Particle identification	3	3	3
Material and interactions	3.5 - 2.5	3.5 - 2.5	4.5 - 2.5
True p_T distribution	3.5 - 1	4.5 - 1	2.5 - 1
Normalisation	0.5	1.5	4.5
Total	17 - 17.5	16.5 - 17	15.5 - 16.5
Uncorrelated	12 - 11.5	11.5 - 10.5	9.5 - 9.5

Table 1: Main contributions to the systematic uncertainty of the $\Lambda(1520)$ p_T -differential yield in 0–20%, 20–50% and 50–80% centrality classes. The values are relative uncertainties (standard deviations expressed in %). When appropriate, they are reported for the lowest and highest measured p_T bin. The total systematic uncertainty and the contribution uncorrelated across centralities (after removing the common uncertainties) are also reported.

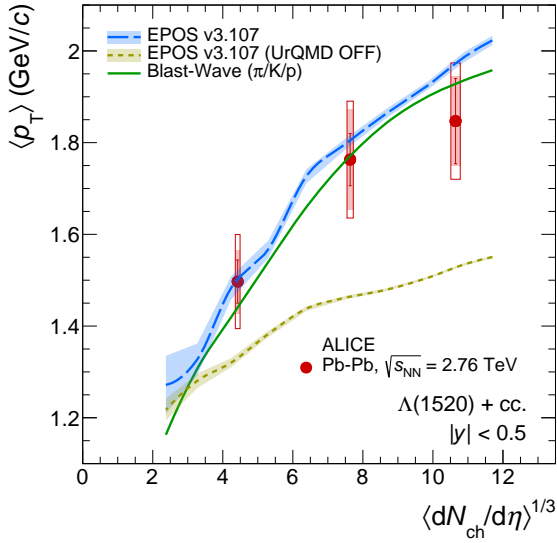


Fig. 3: $\langle p_T \rangle$ of $\Lambda(1520)$ as a function of $\langle dN_{ch}/d\eta \rangle^{1/3}$. Statistical and systematic uncertainties are shown as bars and boxes, respectively. The solid line shows the Blast-Wave predictions. The dashed lines show the predictions from EPOS3 with and without the hadronic phase (UrQMD OFF).

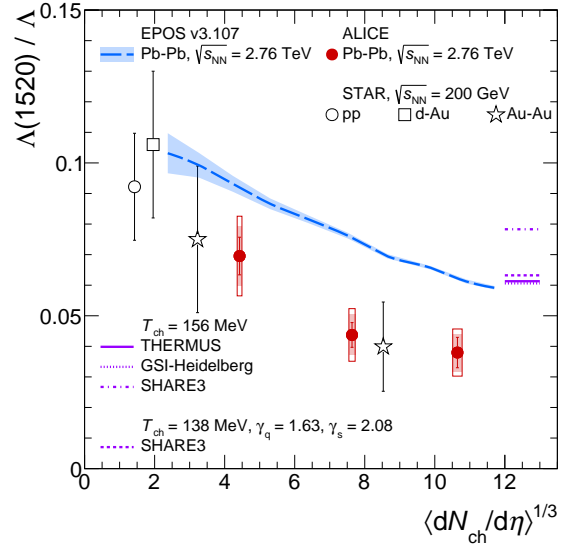


Fig. 4: p_T -integrated ratio of $\Lambda(1520)/\Lambda$ production as a function of $\langle dN_{ch}/d\eta \rangle^{1/3}$. Predictions from several SHMs and from EPOS3 are also shown.

The fully-corrected p_T -differential yields of $\Lambda(1520)$ measured in $|y| < 0.5$ are shown in Fig. 2 in the centrality classes 0–20%, 20–50% and 50–80%. The spectral shapes are compared with predictions from the Blast-Wave model [23], which assumes particle production from thermal sources expanding with a common transverse velocity. The parameters of the model are the ones obtained from published results on pion, kaon and proton production in Pb–Pb collisions [24]. The good agreement of the Blast-Wave predictions with the data is consistent with the scenario where $\Lambda(1520)$ undergoes a similar hydrodynamic evolution as pions, kaons and protons with a common transverse expansion velocity that increases with centrality. The p_T distributions are also compared to predictions of the EPOS3 model [11], a Monte Carlo generator founded on parton-based Gribov-Regge theory, which describes the full evolution of a heavy-ion collision. The model employs viscous hydrodynamic calculations for the description of the expansion of the bulk partonic matter. EPOS3 incorporates the UrQMD [25, 26] transport model to describe the interactions among particles in the hadronic phase in a microscopic approach. The results from the model are in rather good agreement with the measured $\Lambda(1520)$ spectral shapes in all centrality classes, but the model overestimates the yields in central (0–20%) and semi-central (20–50%) collisions.

The p_T -integrated yield, dN/dy , and the average transverse momentum, $\langle p_T \rangle$, are computed by integrating the data and using extrapolations to estimate the yields in the unmeasured regions. The extrapolations

	dN/dy	$\Lambda(1520)/\Lambda$	$\langle p_T \rangle$ (GeV/c)
0–20%	$1.56 \pm 0.20 \pm 0.27$ (0.19)	$0.038 \pm 0.005 \pm 0.008$ (0.006)	$1.85 \pm 0.09 \pm 0.13$ (0.10)
20–50%	$0.70 \pm 0.06 \pm 0.12$ (0.08)	$0.044 \pm 0.004 \pm 0.009$ (0.007)	$1.76 \pm 0.06 \pm 0.13$ (0.11)
50–80%	$0.22 \pm 0.02 \pm 0.03$ (0.02)	$0.069 \pm 0.006 \pm 0.013$ (0.010)	$1.50 \pm 0.05 \pm 0.10$ (0.07)

Table 2: $\Lambda(1520)$ integrated yields, p_T -integrated ratio of $\Lambda(1520)/\Lambda$, $\langle p_T \rangle$ of $\Lambda(1520)$ production and corresponding uncertainties in 0–20%, 20–50% and 50–80% centrality classes. The first and second uncertainties indicate the statistical and total systematic error, respectively. The values in parenthesis show the systematic uncertainty excluding the contributions common to all centrality classes.

are obtained using the best fit of the Blast-Wave function to the p_T distributions. Several other fit functions (Maxwell-Boltzmann, Fermi-Dirac, m_T -exponential, p_T -exponential) are employed to estimate the systematic uncertainties. The fraction of the extrapolated yields are 6.2%, 6.2% and 10.4% for 0–20%, 20–50% and 50–80% centrality events. The total dN/dy systematic uncertainties are 17.2%, 16.5% and 15.6%, with a significant contribution common to all centrality classes of about 12%. The total systematic uncertainties on $\langle p_T \rangle$ are 6.9%, 7.2% and 6.9%. The values of dN/dy and $\langle p_T \rangle$ for $\Lambda(1520)$ are reported in Tab 2.

The ratio of the p_T -integrated yield of $\Lambda(1520)$ to that of its stable counterpart, Λ , highlights the characteristics of resonance production directly related to the particle lifetime, as possible effects due to valence-quark composition cancel. The yields of Λ have been previously measured by ALICE in Pb–Pb collisions at $\sqrt{s_{NN}} = 2.76$ TeV [27]. Since the centrality classes for $\Lambda(1520)$ are different from those of the measured Λ yields, the latter have been interpolated from the measured values fitting their dependence on the number of participating nucleons in the collisions (N_{part}) with the empirical parametrisation $a + b\langle N_{part} \rangle^c$, where a , b and c are free parameters. Moreover, the $\bar{\Lambda}$ yield, which was not published in [27], has been assumed equal to that of Λ , as expected at LHC energies [24]. In the following, Λ refers to the sum of particle and antiparticle states, except for ALICE where it is defined as 2Λ . The yield ratios $\Lambda(1520)/\Lambda$ are reported in Tab. 2.

Figure 3 and 4, respectively, present the $\langle p_T \rangle$ of $\Lambda(1520)$ and the $\Lambda(1520)/\Lambda$ yield ratios as a function of the cubic root of the charged-particle multiplicity density at mid-rapidity [17], $\langle dN_{ch}/d\eta \rangle^{1/3}$. The latter is used as a proxy for the system radius to emphasise the system-size dependence of $\Lambda(1520)$ production, as suggested by femtoscopic studies using Bose-Einstein correlations [28]. The $\langle p_T \rangle$ increases significantly with increasing charged-particle multiplicity, hence with increasing collision centrality (Fig. 3). The value in central (0–20%) collisions is 23% higher than the one in peripheral (50–80%) collisions. The measured $\langle p_T \rangle$ is compared to the prediction from the Blast-Wave model discussed previously [23, 24]. The good agreement further stresses the consistency of the $\Lambda(1520)$ data with a common hydrodynamic evolution picture. The $\langle p_T \rangle$ results also highlight the good agreement with the prediction from the EPOS3 [11] model. It is noteworthy that EPOS3 fails to describe the data when the UrQMD transport stage is disabled, underlining the importance of the latter in the description of the evolution of heavy-ion collisions.

A gradual decrease of the $\Lambda(1520)/\Lambda$ yield ratio with increasing charged-particle multiplicity is observed from peripheral to central Pb–Pb collisions (Fig. 4). The $\Lambda(1520)$ suppression in central Pb–Pb events with respect to peripheral events is measured as the double ratio

$$\frac{[\Lambda(1520)/\Lambda]_{0-20\%}}{[\Lambda(1520)/\Lambda]_{50-80\%}} = 0.54 \pm 0.08 \text{ (stat)} \pm 0.12 \text{ (syst)},$$

where common uncertainties cancel. $\Lambda(1520)/\Lambda$ in central collisions is about 45% lower than in peripheral collisions. The result provides the first evidence for $\Lambda(1520)$ suppression in heavy-ion collisions, with a 3.1σ confidence level. The ratio is compared to grand-canonical equilibrium predictions from the GSI-Heidelberg [4], THERMUS [29] and SHARE3 [30] models, whose parameters have been determined from fits to stable particles [31]. The ratio is also compared to the non-equilibrium configuration implemented in SHARE3, where the under(over)-saturation parameters γ_s (strange) and γ_q (light quarks) are free [32]. All models describe the yield of stable hadrons well. $\Lambda(1520)/\Lambda$ in central collisions is lower than SHM predictions by values ranging from 37% to 52%, depending on the reference model. Figure 4 also shows the data from the STAR Collaboration at RHIC in Au–Au, d–Au and pp collisions at $\sqrt{s_{NN}} = 200$ GeV [13, 14]. The trend of the suppression is similar to the one seen from STAR data in Au–Au collisions at $\sqrt{s_{NN}} = 200$ GeV. The current measurement of $\Lambda(1520)$ suppression has a higher precision at 3.1σ confidence level, as compared to the 1.8σ confidence level of STAR data in Au–Au collisions. Finally, the multiplicity-dependence of the $\Lambda(1520)/\Lambda$ ratio is compared with the prediction

from EPOS3 [11] (Fig. 4). It is important to note that the model, although it systematically overestimates the data, describes the trend of the suppression well. These observations highlight the relevance of the hadronic phase in the study of heavy-ion collisions and the importance of a microscopic description of the late hadronic interactions.

In conclusion, the first measurement of $\Lambda(1520)$ production in Pb–Pb collisions at $\sqrt{s_{NN}} = 2.76$ TeV at the LHC has been presented. The spectral shapes and $\langle p_T \rangle$ are consistent with the hydrodynamic evolution picture that describes pions, kaons and protons, indicating that the $\Lambda(1520)$ experiences the same collective radial expansion, with a common transverse velocity which increases with collision centrality. The comparison of the $\langle p_T \rangle$ results to EPOS3 predictions highlights the relevance of the hadronic phase in the study of heavy-ion collisions and the importance of a microscopic description of the late hadronic interactions. The p_T -integrated ratio $\Lambda(1520)/\Lambda$ is suppressed in central Pb–Pb collisions with respect to peripheral Pb–Pb collisions and is lower than the value predicted by statistical hadronisation models. The measurement adds further support to the formation of a dense hadronic phase in the latest stages of the evolution of the fireball created in high-energy heavy-ion collisions, lasting long enough to cause a significant reduction in the observable yield of short-lived resonances.

Acknowledgements

The ALICE Collaboration would like to thank all its engineers and technicians for their invaluable contributions to the construction of the experiment and the CERN accelerator teams for the outstanding performance of the LHC complex. The ALICE Collaboration gratefully acknowledges the resources and support provided by all Grid centres and the Worldwide LHC Computing Grid (WLCG) collaboration. The ALICE Collaboration acknowledges the following funding agencies for their support in building and running the ALICE detector: A. I. Alikhanyan National Science Laboratory (Yerevan Physics Institute) Foundation (ANSL), State Committee of Science and World Federation of Scientists (WFS), Armenia; Austrian Academy of Sciences and Nationalstiftung für Forschung, Technologie und Entwicklung, Austria; Ministry of Communications and High Technologies, National Nuclear Research Center, Azerbaijan; Conselho Nacional de Desenvolvimento Científico e Tecnológico (CNPq), Universidade Federal do Rio Grande do Sul (UFRGS), Financiadora de Estudos e Projetos (Finep) and Fundação de Amparo à Pesquisa do Estado de São Paulo (FAPESP), Brazil; Ministry of Science & Technology of China (MSTC), National Natural Science Foundation of China (NSFC) and Ministry of Education of China (MOEC), China; Ministry of Science and Education, Croatia; Ministry of Education, Youth and Sports of the Czech Republic, Czech Republic; The Danish Council for Independent Research | Natural Sciences, the Carlsberg Foundation and Danish National Research Foundation (DNRF), Denmark; Helsinki Institute of Physics (HIP), Finland; Commissariat à l’Energie Atomique (CEA) and Institut National de Physique Nucléaire et de Physique des Particules (IN2P3) and Centre National de la Recherche Scientifique (CNRS), France; Bundesministerium für Bildung, Wissenschaft, Forschung und Technologie (BMBF) and GSI Helmholtzzentrum für Schwerionenforschung GmbH, Germany; General Secretariat for Research and Technology, Ministry of Education, Research and Religions, Greece; National Research, Development and Innovation Office, Hungary; Department of Atomic Energy Government of India (DAE), Department of Science and Technology, Government of India (DST), University Grants Commission, Government of India (UGC) and Council of Scientific and Industrial Research (CSIR), India; Indonesian Institute of Science, Indonesia; Centro Fermi - Museo Storico della Fisica e Centro Studi e Ricerche Enrico Fermi and Istituto Nazionale di Fisica Nucleare (INFN), Italy; Institute for Innovative Science and Technology, Nagasaki Institute of Applied Science (IIST), Japan Society for the Promotion of Science (JSPS) KAKENHI and Japanese Ministry of Education, Culture, Sports, Science and Technology (MEXT), Japan; Consejo Nacional de Ciencia (CONACYT) y Tecnología, through Fondo de Cooperación Internacional en Ciencia y Tecnología (FONCICYT) and Dirección General de Asuntos del Personal Académico (DGAPA), Mexico; Nederlandse Organisatie voor Wetenschappelijk Onderzoek

(NWO), Netherlands; The Research Council of Norway, Norway; Commission on Science and Technology for Sustainable Development in the South (COMSATS), Pakistan; Pontificia Universidad Católica del Perú, Peru; Ministry of Science and Higher Education and National Science Centre, Poland; Korea Institute of Science and Technology Information and National Research Foundation of Korea (NRF), Republic of Korea; Ministry of Education and Scientific Research, Institute of Atomic Physics and Romanian National Agency for Science, Technology and Innovation, Romania; Joint Institute for Nuclear Research (JINR), Ministry of Education and Science of the Russian Federation and National Research Centre Kurchatov Institute, Russia; Ministry of Education, Science, Research and Sport of the Slovak Republic, Slovakia; National Research Foundation of South Africa, South Africa; Centro de Aplicaciones Tecnológicas y Desarrollo Nuclear (CEADEN), Cubaenergía, Cuba and Centro de Investigaciones Energéticas, Medioambientales y Tecnológicas (CIEMAT), Spain; Swedish Research Council (VR) and Knut & Alice Wallenberg Foundation (KAW), Sweden; European Organization for Nuclear Research, Switzerland; National Science and Technology Development Agency (NSDTA), Suranaree University of Technology (SUT) and Office of the Higher Education Commission under NRU project of Thailand, Thailand; Turkish Atomic Energy Agency (TAEK), Turkey; National Academy of Sciences of Ukraine, Ukraine; Science and Technology Facilities Council (STFC), United Kingdom; National Science Foundation of the United States of America (NSF) and United States Department of Energy, Office of Nuclear Physics (DOE NP), United States of America.

References

- [1] N. Cabibbo and G. Parisi, “Exponential Hadronic Spectrum and Quark Liberation,” *Phys. Lett.* **59B** (1975) 67–69.
- [2] E. Laermann and O. Philipsen, “The Status of lattice QCD at finite temperature,” *Ann. Rev. Nucl. Part. Sci.* **53** (2003) 163–198, arXiv:hep-ph/0303042 [hep-ph].
- [3] B. Müller and J. L. Nagle, “Results from the relativistic heavy ion collider,” *Ann. Rev. Nucl. Part. Sci.* **56** (2006) 93–135, arXiv:nucl-th/0602029 [nucl-th].
- [4] A. Andronic, P. Braun-Munzinger, and J. Stachel, “Hadron production in central nucleus-nucleus collisions at chemical freeze-out,” *Nucl. Phys.* **A772** (2006) 167–199, arXiv:nucl-th/0511071 [nucl-th].
- [5] F. Becattini and R. Fries, “The QCD confinement transition: Hadron formation,” *Landolt-Bornstein* **23** (2010) 208, arXiv:0907.1031 [nucl-th].
- [6] J. Cleymans and K. Redlich, “Unified description of freezeout parameters in relativistic heavy ion collisions,” *Phys. Rev. Lett.* **81** (1998) 5284–5286, arXiv:nucl-th/9808030 [nucl-th].
- [7] A. Andronic, P. Braun-Munzinger, K. Redlich, and J. Stachel, “The thermal model on the verge of the ultimate test: particle production in Pb–Pb collisions at the LHC,” *J. Phys.* **G38** (2011) 124081, arXiv:1106.6321 [nucl-th].
- [8] C. Markert, R. Bellwied, and I. Vitev, “Formation and decay of hadronic resonances in the QGP,” *Phys. Lett.* **B669** (2008) 92–97, arXiv:0807.1509 [nucl-th].
- [9] M. Bleicher and J. Aichelin, “Strange resonance production: Probing chemical and thermal freezeout in relativistic heavy ion collisions,” *Phys. Lett.* **B530** (2002) 81–87, arXiv:hep-ph/0201123 [hep-ph].
- [10] ALICE Collaboration, B. B. Abelev *et al.*, “ $K^*(892)^0$ and $\phi(1020)$ production in Pb–Pb collisions at $\sqrt{s_{NN}} = 2.76$ TeV,” *Phys. Rev.* **C91** (2015) 024609, arXiv:1404.0495 [nucl-ex].

- [11] A. G. Knospe, C. Markert, K. Werner, J. Steinheimer, and M. Bleicher, “Hadronic resonance production and interaction in partonic and hadronic matter in the EPOS3 model with and without the hadronic afterburner UrQMD,” *Phys. Rev.* **C93** no. 1, (2016) 014911, arXiv:1509.07895 [nucl-th].
- [12] ALICE Collaboration, K. Aamodt *et al.*, “The ALICE experiment at the CERN LHC,” *JINST* **3** (2008) S08002.
- [13] STAR Collaboration, B. I. Abelev *et al.*, “Strange baryon resonance production in $\sqrt{s_{NN}} = 200$ GeV p+p and Au+Au collisions,” *Phys. Rev. Lett.* **97** (2006) 132301, arXiv:nucl-ex/0604019 [nucl-ex].
- [14] STAR Collaboration, B. I. Abelev *et al.*, “Hadronic resonance production in d+Au collisions at $\sqrt{s_{NN}} = 200$ GeV at RHIC,” *Phys. Rev.* **C78** (2008) 044906, arXiv:0801.0450 [nucl-ex].
- [15] ALICE Collaboration, B. B. Abelev *et al.*, “Performance of the ALICE Experiment at the CERN LHC,” *Int. J. Mod. Phys.* **A29** (2014) 1430044, arXiv:1402.4476 [nucl-ex].
- [16] ALICE Collaboration, K. Aamodt *et al.*, “Charged-particle multiplicity density at mid-rapidity in central Pb–Pb collisions at $\sqrt{s_{NN}} = 2.76$ TeV,” *Phys. Rev. Lett.* **105** (2010) 252301, arXiv:1011.3916 [nucl-ex].
- [17] ALICE Collaboration, K. Aamodt *et al.*, “Centrality dependence of the charged-particle multiplicity density at mid-rapidity in Pb–Pb collisions at $\sqrt{s_{NN}} = 2.76$ TeV,” *Phys. Rev. Lett.* **106** (2011) 032301, arXiv:1012.1657 [nucl-ex].
- [18] ALICE Collaboration, B. Abelev *et al.*, “Centrality determination of Pb–Pb collisions at $\sqrt{s_{NN}} = 2.76$ TeV with ALICE,” *Phys. Rev.* **C88** no. 4, (2013) 044909, arXiv:1301.4361 [nucl-ex].
- [19] C. Patrignani *et al.*, “Review of Particle Physics,” *Chin. Phys.* **C40** no. 10, (2016) 100001.
- [20] D. L’Hote, “About Resonance signal extraction from multiparticle data: combinatorics and event mixing methods,” *Nucl. Instrum. Meth.* **A337** (1994) 544–556.
- [21] X.-N. Wang and M. Gyulassy, “HIJING: A Monte Carlo model for multiple jet production in p p, p A and A A collisions,” *Phys. Rev.* **D44** (1991) 3501–3516.
- [22] R. Brun, F. Bruyant, F. Carminati, S. Giani, M. Maire, A. McPherson, G. Patrick, and L. Urban, “GEANT Detector Description and Simulation Tool,” <http://cds.cern.ch/record/1082634>.
- [23] E. Schnedermann, J. Sollfrank, and U. W. Heinz, “Thermal phenomenology of hadrons from 200-A/GeV S+S collisions,” *Phys. Rev.* **C48** (1993) 2462–2475, arXiv:nucl-th/9307020 [nucl-th].
- [24] ALICE Collaboration, B. Abelev *et al.*, “Centrality dependence of π , K, p production in Pb–Pb collisions at $\sqrt{s_{NN}} = 2.76$ TeV,” *Phys. Rev.* **C88** (2013) 044910, arXiv:1303.0737 [hep-ex].
- [25] S. A. Bass *et al.*, “Microscopic models for ultrarelativistic heavy ion collisions,” *Prog. Part. Nucl. Phys.* **41** (1998) 255–369, arXiv:nucl-th/9803035 [nucl-th].
- [26] M. Bleicher *et al.*, “Relativistic hadron hadron collisions in the ultrarelativistic quantum molecular dynamics model,” *J. Phys.* **G25** (1999) 1859–1896, arXiv:hep-ph/9909407 [hep-ph].
- [27] ALICE Collaboration, B. B. Abelev *et al.*, “ K_S^0 and Λ production in Pb–Pb collisions at $\sqrt{s_{NN}} = 2.76$ TeV,” *Phys. Rev. Lett.* **111** (2013) 222301, arXiv:1307.5530 [nucl-ex].

- [28] ALICE Collaboration, K. Aamodt *et al.*, “Two-pion Bose-Einstein correlations in central Pb–Pb collisions at $\sqrt{s_{\text{NN}}} = 2.76$ TeV,” *Phys. Lett.* **B696** (2011) 328–337, arXiv:1012.4035 [nucl-ex].
- [29] S. Wheaton and J. Cleymans, “Statistical-thermal model calculations using THERMUS,” *J. Phys.* **G31** (2005) S1069–S1074, arXiv:hep-ph/0412031 [hep-ph].
- [30] M. Petran, J. Letessier, J. Rafelski, and G. Torrieri, “SHARE with CHARM,” *Comput. Phys. Commun.* **185** (2014) 2056–2079, arXiv:1310.5108 [hep-ph].
- [31] M. Floris, “Hadron yields and the phase diagram of strongly interacting matter,” *Nucl. Phys.* **A931** (2014) 103–112, arXiv:1408.6403 [nucl-ex].
- [32] M. Petran, J. Letessier, V. Petraek, and J. Rafelski, “Hadron production and quark-gluon plasma hadronization in Pb–Pb collisions at $\sqrt{s_{\text{NN}}} = 2.76$ TeV,” *Phys. Rev.* **C88** no. 3, (2013) 034907, arXiv:1303.2098 [hep-ph].

A The ALICE Collaboration

S. Acharya¹³⁸, F.T.-. Acosta²², D. Adamová⁹⁴, J. Adolfsson⁸¹, M.M. Aggarwal⁹⁸, G. Aglieri Rinella³⁶, M. Agnello³³, N. Agrawal⁴⁹, Z. Ahammed¹³⁸, S.U. Ahn⁷⁷, S. Aiola¹⁴³, A. Akindinov⁶⁵, M. Al-Turany¹⁰⁴, S.N. Alam¹³⁸, D.S.D. Albuquerque¹²⁰, D. Aleksandrov⁸⁸, B. Alessandro⁵⁹, R. Alfaro Molina⁷³, Y. Ali¹⁶, A. Alici^{11, 54, 29}, A. Alkin³, J. Alme²⁴, T. Alt⁷⁰, L. Altenkamper²⁴, I. Altsybeev¹³⁷, M.N. Anaam⁷, C. Andrei⁴⁸, D. Andreou³⁶, H.A. Andrews¹⁰⁸, A. Andronic^{141, 104}, M. Angeletti³⁶, V. Anguelov¹⁰², C. Anson¹⁷, T. Antičić¹⁰⁵, F. Antinori⁵⁷, P. Antonioli⁵⁴, R. Anwar¹²⁴, N. Apadula⁸⁰, L. Aphecetche¹¹², H. Appelshäuser⁷⁰, S. Arce²⁹, R. Arnaldi⁵⁹, O.W. Arnold^{103, 115}, I.C. Arsene²³, M. Arslanok¹⁰², B. Audurier¹¹², A. Augustinus³⁶, R. Averbeck¹⁰⁴, M.D. Azmi¹⁸, A. Badalà⁵⁶, Y.W. Baek^{61, 42}, S. Bagnasco⁵⁹, R. Bailhache⁷⁰, R. Bala⁹⁹, A. Baldisseri¹³⁴, M. Ball⁴⁴, R.C. Baral⁸⁶, A.M. Barbano²⁸, R. Barbera³⁰, F. Barile⁵³, L. Barioglio²⁸, G.G. Barnaföldi¹⁴², L.S. Barnby⁹³, V. Barret¹³¹, P. Bartalini⁷, K. Barth³⁶, E. Bartsch⁷⁰, N. Bastid¹³¹, S. Basu¹⁴⁰, G. Batigne¹¹², B. Batyunya⁷⁶, P.C. Batzing²³, J.L. Bazo Alba¹⁰⁹, I.G. Bearden⁸⁹, H. Beck¹⁰², C. Bedda⁶⁴, N.K. Behera⁶¹, I. Belikov¹³³, F. Bellini³⁶, H. Bello Martinez², R. Bellwied¹²⁴, L.G.E. Beltran¹¹⁸, V. Belyaev⁹², G. Bencedi¹⁴², S. Beole²⁸, A. Bercuci⁴⁸, Y. Berdnikov⁹⁶, D. Berenyi¹⁴², R.A. Bertens¹²⁷, D. Berzano^{36, 59}, L. Betev³⁶, P.P. Bhaduri¹³⁸, A. Bhasin⁹⁹, I.R. Bhat⁹⁹, H. Bhatt⁴⁹, B. Bhattacharjee⁴³, J. Bhowmik¹¹⁶, A. Bianchi²⁸, L. Bianchi¹²⁴, N. Bianchi⁵², J. Bielčik³⁹, J. Bielčiková⁹⁴, A. Bilandzic^{115, 103}, G. Biro¹⁴², R. Biswas⁴, S. Biswas⁴, J.T. Blair¹¹⁷, D. Blau⁸⁸, C. Blume⁷⁰, G. Boca¹³⁵, F. Bock³⁶, A. Bogdanov⁹², L. Boldizsár¹⁴², M. Bombara⁴⁰, G. Bonomi¹³⁶, M. Bonora³⁶, H. Borel¹³⁴, A. Borissov^{20, 141}, M. Borri¹²⁶, E. Botta²⁸, C. Bourjau⁸⁹, L. Bratrud⁷⁰, P. Braun-Munzinger¹⁰⁴, M. Bregant¹¹⁹, T.A. Broker⁷⁰, M. Broz³⁹, E.J. Brucken⁴⁵, E. Bruna⁵⁹, G.E. Bruno^{36, 35}, D. Budnikov¹⁰⁶, H. Buesching⁷⁰, S. Bufalino³³, P. Buhler¹¹¹, P. Buncic³⁶, O. Busch^{130, i}, Z. Buthelezi⁷⁴, J.B. Butt¹⁶, J.T. Buxton¹⁹, J. Cabala¹¹⁴, D. Caffarri⁹⁰, H. Caines¹⁴³, A. Caliva¹⁰⁴, E. Calvo Villar¹⁰⁹, R.S. Camacho², P. Camerini²⁷, A.A. Capon¹¹¹, F. Carena³⁶, W. Carena³⁶, F. Carnesecchi^{29, 11}, J. Castillo Castellanos¹³⁴, A.J. Castro¹²⁷, E.A.R. Casula⁵⁵, C. Ceballos Sanchez⁹, S. Chandra¹³⁸, B. Chang¹²⁵, W. Chang⁷, S. Chapeland³⁶, M. Chartier¹²⁶, S. Chattopadhyay¹³⁸, S. Chattopadhyay¹⁰⁷, A. Chauvin^{103, 115}, C. Cheshkov¹³², B. Cheynis¹³², V. Chibante Barroso³⁶, D.D. Chinellato¹²⁰, S. Cho⁶¹, P. Chochula³⁶, T. Chowdhury¹³¹, P. Christakoglou⁹⁰, C.H. Christensen⁸⁹, P. Christiansen⁸¹, T. Chujo¹³⁰, S.U. Chung²⁰, C. Cicalo⁵⁵, L. Cifarelli^{11, 29}, F. Cindolo⁵⁴, J. Cleymans¹²³, F. Colamaria⁵³, D. Colella^{66, 36, 53}, A. Collu⁸⁰, M. Colocci²⁹, M. Concas^{59, ii}, G. Conesa Balbastre⁷⁹, Z. Conesa del Valle⁶², J.G. Contreras³⁹, T.M. Cormier⁹⁵, Y. Corrales Morales⁵⁹, P. Cortese³⁴, M.R. Cosentino¹²¹, F. Costa³⁶, S. Costanza¹³⁵, J. Crkovská⁶², P. Crochet¹³¹, E. Cuautle⁷¹, L. Cunqueiro^{141, 95}, T. Dahms^{103, 115}, A. Dainese⁵⁷, S. Dani⁶⁷, M.C. Danisch¹⁰², A. Danu⁶⁹, D. Das¹⁰⁷, I. Das¹⁰⁷, S. Das⁴, A. Dash⁸⁶, S. Dash⁴⁹, S. De⁵⁰, A. De Caro³², G. de Cataldo⁵³, C. de Conti¹¹⁹, J. de Cuveland⁴¹, A. De Falco²⁶, D. De Gruttola^{11, 32}, N. De Marco⁵⁹, S. De Pasquale³², R.D. De Souza¹²⁰, H.F. Degenhardt¹¹⁹, A. Deisting^{104, 102}, A. Deloff⁸⁵, S. Delsanto²⁸, C. Deplano⁹⁰, P. Dhankher⁴⁹, D. Di Bari³⁵, A. Di Mauro³⁶, B. Di Ruzza⁵⁷, R.A. Diaz⁹, T. Dietel¹²³, P. Dillenseger⁷⁰, Y. Ding⁷, R. Divià³⁶, Ø. Djuvsland²⁴, A. Dobrin³⁶, D. Domenicis Gimenez¹¹⁹, B. Dönigus⁷⁰, O. Dordic²³, L.V.R. Doremalen⁶⁴, A.K. Dubey¹³⁸, A. Dubla¹⁰⁴, L. Ducroux¹³², S. Dudi⁹⁸, A.K. Duggal⁹⁸, M. Dukhishyam⁸⁶, P. Dupieux¹³¹, R.J. Ehlers¹⁴³, D. Elia⁵³, E. Endress¹⁰⁹, H. Engel⁷⁵, E. Epple¹⁴³, B. Erazmus¹¹², F. Erhardt⁹⁷, M.R. Ernsdal²⁴, B. Espagnon⁶², G. Eulisse³⁶, J. Eum²⁰, D. Evans¹⁰⁸, S. Evdokimov⁹¹, L. Fabbietti^{103, 115}, M. Faggin³¹, J. Faivre⁷⁹, A. Fantoni⁵², M. Fasel⁹⁵, L. Feldkamp¹⁴¹, A. Feliciello⁵⁹, G. Feofilov¹³⁷, A. Fernández Téllez², A. Ferretti²⁸, A. Festanti^{31, 36}, V.J.G. Feuillard¹⁰², J. Figiel¹¹⁶, M.A.S. Figueredo¹¹⁹, S. Filchagin¹⁰⁶, D. Finogeev⁶³, F.M. Fionda²⁴, G. Fiorenza⁵³, F. Flor¹²⁴, M. Floris³⁶, S. Foertsch⁷⁴, P. Foka¹⁰⁴, S. Fokin⁸⁸, E. Fragiaco⁶⁰, A. Francescon³⁶, A. Francisco¹¹², U. Frankenfeld¹⁰⁴, G.G. Fronze²⁸, U. Fuchs³⁶, C. Furget⁷⁹, A. Furs⁶³, M. Fusco Girard³², J.J. Gaardhøje⁸⁹, M. Gagliardi²⁸, A.M. Gago¹⁰⁹, K. Gajdosova⁸⁹, M. Gallio²⁸, C.D. Galvan¹¹⁸, P. Ganoti⁸⁴, C. Garabatos¹⁰⁴, E. Garcia-Solis¹², K. Garg³⁰, C. Gargiulo³⁶, P. Gasik^{115, 103}, E.F. Gauger¹¹⁷, M.B. Gay Ducati⁷², M. Germain¹¹², J. Ghosh¹⁰⁷, P. Ghosh¹³⁸, S.K. Ghosh⁴, P. Gianotti⁵², P. Giubellino^{104, 59}, P. Giubileo³¹, P. Glässel¹⁰², D.M. Gómez Coral⁷³, A. Gomez Ramirez⁷⁵, V. Gonzalez¹⁰⁴, P. González-Zamora², S. Gorbunov⁴¹, L. Görlich¹¹⁶, S. Gotovac³⁷, V. Grabski⁷³, L.K. Graczykowski¹³⁹, K.L. Graham¹⁰⁸, L. Greiner⁸⁰, A. Grelli⁶⁴, C. Grigoras³⁶, V. Grigoriev⁹², A. Grigoryan¹, S. Grigoryan⁷⁶, J.M. Gronefeld¹⁰⁴, F. Grosa³³, J.F. Grosse-Oetringhaus³⁶, R. Grosso¹⁰⁴, R. Guernane⁷⁹, B. Guerzoni²⁹, M. Guittiere¹¹², K. Gulbrandsen⁸⁹, T. Gunji¹²⁹, A. Gupta⁹⁹, R. Gupta⁹⁹, I.B. Guzman², R. Haake³⁶, M.K. Habib¹⁰⁴, C. Hadjidakis⁶², H. Hamagaki⁸², G. Hamar¹⁴², M. Hamid⁷, J.C. Hamon¹³³, R. Hannigan¹¹⁷, M.R. Haque⁶⁴, J.W. Harris¹⁴³, A. Harton¹², H. Hassan⁷⁹, D. Hatzifotiadou^{54, 11}, S. Hayashi¹²⁹, S.T. Heckel⁷⁰, E. Hellbär⁷⁰, H. Helstrup³⁸, A. Hergelegiu⁴⁸, E.G. Hernandez², G. Herrera Corral¹⁰, F. Herrmann¹⁴¹, K.F. Hetland³⁸, T.E. Hilden⁴⁵, H. Hillemanns³⁶, C. Hills¹²⁶, B. Hippolyte¹³³, B. Hohlweger¹⁰², D. Horak³⁹, S. Hornung¹⁰⁴, R. Hosokawa^{130, 79}, J. Hota⁶⁷,

P. Hristov³⁶, C. Huang⁶², C. Hughes¹²⁷, P. Huhn⁷⁰, T.J. Humanic¹⁹, H. Hushnud¹⁰⁷, N. Hussain⁴³, T. Hussain¹⁸, D. Hutter⁴¹, D.S. Hwang²¹, J.P. Iddon¹²⁶, S.A. Iga Buitron⁷¹, R. Ilkaev¹⁰⁶, M. Inaba¹³⁰, M. Ippolitov⁸⁸, M.S. Islam¹⁰⁷, M. Ivanov¹⁰⁴, V. Ivanov⁹⁶, V. Izucheev⁹¹, B. Jacak⁸⁰, N. Jacazio²⁹, P.M. Jacobs⁸⁰, M.B. Jadhav⁴⁹, S. Jadlovská¹¹⁴, J. Jadlovsky¹¹⁴, S. Jaelani⁶⁴, C. Jahnke^{119,115}, M.J. Jakubowska¹³⁹, M.A. Janik¹³⁹, C. Jena⁸⁶, M. Jercic⁹⁷, O. Jevons¹⁰⁸, R.T. Jimenez Bustamante¹⁰⁴, M. Jin¹²⁴, P.G. Jones¹⁰⁸, A. Jusko¹⁰⁸, P. Kalinak⁶⁶, A. Kalweit³⁶, J.H. Kang¹⁴⁴, V. Kaplin⁹², S. Kar⁷, A. Karasu Uysal⁷⁸, O. Karavichev⁶³, T. Karavicheva⁶³, P. Karczmarczyk³⁶, E. Karpechev⁶³, U. Kebschull⁷⁵, R. Keidel⁴⁷, D.L.D. Keijdener⁶⁴, M. Keil³⁶, B. Ketzer⁴⁴, Z. Khabanova⁹⁰, A.M. Khan⁷, S. Khan¹⁸, S.A. Khan¹³⁸, A. Khanzadeev⁹⁶, Y. Kharlov⁹¹, A. Khatun¹⁸, A. Khuntia⁵⁰, M.M. Kielbowicz¹¹⁶, B. Kileng³⁸, B. Kim¹³⁰, D. Kim¹⁴⁴, D.J. Kim¹²⁵, E.J. Kim¹⁴, H. Kim¹⁴⁴, J.S. Kim⁴², J. Kim¹⁰², M. Kim^{61,102}, S. Kim²¹, T. Kim¹⁴⁴, T. Kim¹⁴⁴, S. Kirsch⁴¹, I. Kisel⁴¹, S. Kiselev⁶⁵, A. Kisiel¹³⁹, J.L. Klay⁶, C. Klein⁷⁰, J. Klein^{36,59}, C. Klein-Bösing¹⁴¹, S. Klewin¹⁰², A. Kluge³⁶, M.L. Knichel³⁶, A.G. Knospe¹²⁴, C. Kobdaj¹¹³, M. Kofarago¹⁴², M.K. Köhler¹⁰², T. Kollegger¹⁰⁴, N. Kondratyeva⁹², E. Kondratyuk⁹¹, A. Konevskikh⁶³, M. Konyushikhin¹⁴⁰, O. Kovalenko⁸⁵, V. Kovalenko¹³⁷, M. Kowalski¹¹⁶, I. Králik⁶⁶, A. Kravčáková⁴⁰, L. Kreis¹⁰⁴, M. Krivda^{66,108}, F. Krizek⁹⁴, M. Krüger⁷⁰, E. Kryshen⁹⁶, M. Krzewicki⁴¹, A.M. Kubera¹⁹, V. Kučera^{94,61}, C. Kuhn¹³³, P.G. Kuijjer⁹⁰, J. Kumar⁴⁹, L. Kumar⁹⁸, S. Kumar⁴⁹, S. Kundu⁸⁶, P. Kurashvili⁸⁵, A. Kurepin⁶³, A.B. Kurepin⁶³, A. Kuryakin¹⁰⁶, S. Kushpil⁹⁴, J. Kvapil¹⁰⁸, M.J. Kweon⁶¹, Y. Kwon¹⁴⁴, S.L. La Pointe⁴¹, P. La Rocca³⁰, Y.S. Lai⁸⁰, I. Lakomov³⁶, R. Langoy¹²², K. Lapidus¹⁴³, C. Lara⁷⁵, A. Lardeux²³, P. Larionov⁵², E. Laudi³⁶, R. Lavicka³⁹, R. Lea²⁷, L. Leardini¹⁰², S. Lee¹⁴⁴, F. Lehas⁹⁰, S. Lehner¹¹¹, J. Lehrbach⁴¹, R.C. Lemmon⁹³, I. León Monzón¹¹⁸, P. Lévai¹⁴², X. Li¹³, X.L. Li⁷, J. Lien¹²², R. Lietava¹⁰⁸, B. Lim²⁰, S. Lindal²³, V. Lindenstruth⁴¹, S.W. Lindsay¹²⁶, C. Lippmann¹⁰⁴, M.A. Lisa¹⁹, V. Litichevskiy⁴⁵, A. Liu⁸⁰, H.M. Ljunggren⁸¹, W.J. Llope¹⁴⁰, D.F. Lodato⁶⁴, V. Loginov⁹², C. Loizides^{95,80}, P. Loncar³⁷, X. Lopez¹³¹, E. López Torres⁹, A. Lowe¹⁴², P. Luettig⁷⁰, J.R. Luhder¹⁴¹, M. Lunardon³¹, G. Luparello⁶⁰, M. Lupi³⁶, A. Maevskaya⁶³, M. Mager³⁶, S.M. Mahmood²³, A. Maire¹³³, R.D. Majka¹⁴³, M. Malaev⁹⁶, Q.W. Malik²³, L. Malinina^{76,iii}, D. Mal'Kevich⁶⁵, P. Malzacher¹⁰⁴, A. Mamonov¹⁰⁶, V. Manko⁸⁸, F. Manso¹³¹, V. Manzari⁵³, Y. Mao⁷, M. Marchisone^{74,128,132}, J. Mareš⁶⁸, G.V. Margagliotti²⁷, A. Margotti⁵⁴, J. Margutti⁶⁴, A. Marín¹⁰⁴, C. Markert¹¹⁷, M. Marquard⁷⁰, N.A. Martin¹⁰⁴, P. Martinengo³⁶, J.L. Martinez¹²⁴, M.I. Martínez², G. Martínez García¹¹², M. Martinez Pedreira³⁶, S. Masciocchi¹⁰⁴, M. Maserà²⁸, A. Masoni⁵⁵, L. Massacrier⁶², E. Masson¹¹², A. Mastroserio⁵³, A.M. Mathis^{103,115}, P.F.T. Matuoka¹¹⁹, A. Matyjka^{127,116}, C. Mayer¹¹⁶, M. Mazzilli³⁵, M.A. Mazzoni⁵⁸, F. Meddi²⁵, Y. Melikyan⁹², A. Menchaca-Rocha⁷³, E. Meninno³², J. Mercado Pérez¹⁰², M. Meres¹⁵, C.S. Meza¹⁰⁹, S. Mhlanga¹²³, Y. Miake¹³⁰, L. Micheletti²⁸, M.M. Mieskolainen⁴⁵, D.L. Mihaylov¹⁰³, K. Mikhaylov^{65,76}, A. Mischke⁶⁴, A.N. Mishra⁷¹, D. Miśkowiec¹⁰⁴, J. Mitra¹³⁸, C.M. Mitu⁶⁹, N. Mohammadi³⁶, A.P. Mohanty⁶⁴, B. Mohanty⁸⁶, M. Mohisin Khan^{18,iv}, D.A. Moreira De Godoy¹⁴¹, L.A.P. Moreno², S. Moretto³¹, A. Morreale¹¹², A. Morsch³⁶, V. Muccifora⁵², E. Mudnic³⁷, D. Mühlheim¹⁴¹, S. Muhuri¹³⁸, M. Mukherjee⁴, J.D. Mulligan¹⁴³, M.G. Munhoz¹¹⁹, K. Mürning⁴⁴, M.I.A. Muñoz⁸⁰, R.H. Munzer⁷⁰, H. Murakami¹²⁹, S. Murray⁷⁴, L. Musa³⁶, J. Musinsky⁶⁶, C.J. Myers¹²⁴, J.W. Myrcha¹³⁹, B. Naik⁴⁹, R. Nair⁸⁵, B.K. Nandi⁴⁹, R. Nania^{54,11}, E. Nappi⁵³, A. Narayan⁴⁹, M.U. Naru¹⁶, A.F. Nassirpour⁸¹, H. Natal da Luz¹¹⁹, C. Natrass¹²⁷, S.R. Navarro², K. Nayak⁸⁶, R. Nayak⁴⁹, T.K. Nayak¹³⁸, S. Nazarenko¹⁰⁶, R.A. Negrao De Oliveira^{70,36}, L. Nellen⁷¹, S.V. Nesbo³⁸, G. Neskovic⁴¹, F. Ng¹²⁴, M. Nicassio¹⁰⁴, J. Niedziela^{139,36}, B.S. Nielsen⁸⁹, S. Nikolaev⁸⁸, S. Nikulin⁸⁸, V. Nikulin⁹⁶, F. Noferini^{11,54}, P. Nomokonov⁷⁶, G. Nooren⁶⁴, J.C.C. Noris², J. Norman⁷⁹, A. Nyanin⁸⁸, J. Nystrand²⁴, H. Oh¹⁴⁴, A. Ohlson¹⁰², J. Oleniacz¹³⁹, A.C. Oliveira Da Silva¹¹⁹, M.H. Oliver¹⁴³, J. Onderwaater¹⁰⁴, C. Oppedisano⁵⁹, R. Orava⁴⁵, M. Oravec¹¹⁴, A. Ortiz Velasquez⁷¹, A. Oskarsson⁸¹, J. Otwinowski¹¹⁶, K. Oyama⁸², Y. Pachmayer¹⁰², V. Pacik⁸⁹, D. Pagano¹³⁶, G. Paic⁷¹, P. Palni⁷, J. Pan¹⁴⁰, A.K. Pandey⁴⁹, S. Panebianco¹³⁴, V. Papikyan¹, P. Pareek⁵⁰, J. Park⁶¹, J.E. Parkkila¹²⁵, S. Parmar⁹⁸, A. Passfeld¹⁴¹, S.P. Pathak¹²⁴, R.N. Patra¹³⁸, B. Paul⁵⁹, H. Pei⁷, T. Peitzmann⁶⁴, X. Peng⁷, L.G. Pereira⁷², H. Pereira Da Costa¹³⁴, D. Peresunko⁸⁸, E. Perez Lezama⁷⁰, V. Peskov⁷⁰, Y. Pestov⁵, V. Petráček³⁹, M. Petrovici⁴⁸, C. Petta³⁰, R.P. Pezzi⁷², S. Piano⁶⁰, M. Pikna¹⁵, P. Pillot¹¹², L.O.D.L. Pimentel⁸⁹, O. Pinazza^{54,36}, L. Pinsky¹²⁴, S. Pisano⁵², D.B. Piyathana¹²⁴, M. Płoskoń⁸⁰, M. Planinic⁹⁷, F. Pliquett⁷⁰, J. Pluta¹³⁹, S. Pochybova¹⁴², P.L.M. Podesta-Lerma¹¹⁸, M.G. Poghosyan⁹⁵, B. Polichtchouk⁹¹, N. Poljak⁹⁷, W. Poonsawat¹¹³, A. Pop⁴⁸, H. Poppenborg¹⁴¹, S. Porteboeuf-Houssais¹³¹, V. Pozdniakov⁷⁶, S.K. Prasad⁴, R. Preghenella⁵⁴, F. Prino⁵⁹, C.A. Pruneau¹⁴⁰, I. Pshenichnov⁶³, M. Puccio²⁸, V. Punin¹⁰⁶, J. Putschke¹⁴⁰, S. Raha⁴, S. Rajput⁹⁹, J. Rak¹²⁵, A. Rakotozafindrabe¹³⁴, L. Ramello³⁴, F. Rami¹³³, R. Raniwala¹⁰⁰, S. Raniwala¹⁰⁰, S.S. Räsänen⁴⁵, B.T. Rascanu⁷⁰, V. Ratza⁴⁴, I. Ravasenga³³, K.F. Read^{127,95}, K. Redlich^{85,v}, A. Rehman²⁴, P. Reichelt⁷⁰, F. Reidt³⁶, X. Ren⁷, R. Renfordt⁷⁰, A. Reshetin⁶³, J.-P. Revol¹¹, K. Reygers¹⁰², V. Riabov⁹⁶, T. Richert^{64,81}, M. Richter²³, P. Riedler³⁶, W. Riegler³⁶, F. Riggi³⁰, C. Ristea⁶⁹, S.P. Rode⁵⁰,

M. Rodríguez Cahuantzi², K. Røed²³, R. Rogalev⁹¹, E. Rogochaya⁷⁶, D. Rohr³⁶, D. Röhrich²⁴, P.S. Rokita¹³⁹, F. Ronchetti⁵², E.D. Rosas⁷¹, K. Roslon¹³⁹, P. Rosnet¹³¹, A. Rossi³¹, A. Rotondi¹³⁵, F. Roukoutakis⁸⁴, C. Roy¹³³, P. Roy¹⁰⁷, O.V. Rueda⁷¹, R. Rui²⁷, B. Rumyantsev⁷⁶, A. Rustamov⁸⁷, E. Ryabinkin⁸⁸, Y. Ryabov⁹⁶, A. Rybicki¹¹⁶, S. Saarinen⁴⁵, S. Sadhu¹³⁸, S. Sadovsky⁹¹, K. Šafařík³⁶, S.K. Saha¹³⁸, B. Sahoo⁴⁹, P. Sahoo⁵⁰, R. Sahoo⁵⁰, S. Sahoo⁶⁷, P.K. Sahu⁶⁷, J. Saini¹³⁸, S. Sakai¹³⁰, M.A. Saleh¹⁴⁰, S. Sambyal⁹⁹, V. Samsonov^{96,92}, A. Sandoval⁷³, A. Sarkar⁷⁴, D. Sarkar¹³⁸, N. Sarkar¹³⁸, P. Sarma⁴³, M.H.P. Sas⁶⁴, E. Scapparone⁵⁴, F. Scarlassara³¹, B. Schaefer⁹⁵, H.S. Scheid⁷⁰, C. Schiaua⁴⁸, R. Schicker¹⁰², C. Schmidt¹⁰⁴, H.R. Schmidt¹⁰¹, M.O. Schmidt¹⁰², M. Schmidt¹⁰¹, N.V. Schmidt^{95,70}, J. Schukraft³⁶, Y. Schutz^{36,133}, K. Schwarz¹⁰⁴, K. Schweda¹⁰⁴, G. Scioli²⁹, E. Scomparin⁵⁹, M. Šefčík⁴⁰, J.E. Seger¹⁷, Y. Sekiguchi¹²⁹, D. Sekihata⁴⁶, I. Selyuzhenkov^{104,92}, K. Senosi⁷⁴, S. Senyukov¹³³, E. Serradilla⁷³, P. Sett⁴⁹, A. Sevcenco⁶⁹, A. Shabanov⁶³, A. Shabetai¹¹², R. Shahoyan³⁶, W. Shaikh¹⁰⁷, A. Shangaraev⁹¹, A. Sharma⁹⁸, A. Sharma⁹⁹, M. Sharma⁹⁹, N. Sharma⁹⁸, A.I. Sheikh¹³⁸, K. Shigaki⁴⁶, M. Shimomura⁸³, S. Shirinkin⁶⁵, Q. Shou^{7,110}, K. Shtejer²⁸, Y. Sibiriak⁸⁸, S. Siddhanta⁵⁵, K.M. Sielewicz³⁶, T. Siemiarczuk⁸⁵, D. Silvermyr⁸¹, G. Simatovic⁹⁰, G. Simonetti^{36,103}, R. Singaraju¹³⁸, R. Singh⁸⁶, R. Singh⁹⁹, V. Singhal¹³⁸, T. Sinha¹⁰⁷, B. Sitar¹⁵, M. Sitta³⁴, T.B. Skaali²³, M. Slupecki¹²⁵, N. Smirnov¹⁴³, R.J.M. Snellings⁶⁴, T.W. Snellman¹²⁵, J. Song²⁰, F. Soramel³¹, S. Sorensen¹²⁷, F. Sozzi¹⁰⁴, I. Sputowska¹¹⁶, J. Stachel¹⁰², I. Stan⁶⁹, P. Stankus⁹⁵, E. Stenlund⁸¹, D. Stocco¹¹², M.M. Storetvedt³⁸, P. Strmen¹⁵, A.A.P. Suaide¹¹⁹, T. Sugitate⁴⁶, C. Suire⁶², M. Suleymanov¹⁶, M. Suljic^{36,27}, R. Sultanov⁶⁵, M. Šumbera⁹⁴, S. Sumowidagdo⁵¹, K. Suzuki¹¹¹, S. Swain⁶⁷, A. Szabo¹⁵, I. Szarka¹⁵, U. Tabassam¹⁶, J. Takahashi¹²⁰, G.J. Tambave²⁴, N. Tanaka¹³⁰, M. Tarhini¹¹², M. Tariq¹⁸, M.G. Tarzila⁴⁸, A. Tauro³⁶, G. Tejada Muñoz², A. Telesca³⁶, C. Terrevoli³¹, B. Teyssier¹³², D. Thakur⁵⁰, S. Thakur¹³⁸, D. Thomas¹¹⁷, F. Thoresen⁸⁹, R. Tieulent¹³², A. Tikhonov⁶³, A.R. Timmins¹²⁴, A. Toia⁷⁰, N. Topilskaya⁶³, M. Toppi⁵², S.R. Torres¹¹⁸, S. Tripathy⁵⁰, S. Trogolo²⁸, G. Trombetta³⁵, L. Tropp⁴⁰, V. Trubnikov³, W.H. Trzaska¹²⁵, T.P. Trzcinski¹³⁹, B.A. Trzeciak⁶⁴, T. Tsuji¹²⁹, A. Tumkin¹⁰⁶, R. Turrisi⁵⁷, T.S. Tveter²³, K. Ullaland²⁴, E.N. Umaka¹²⁴, A. Uras¹³², G.L. Usai²⁶, A. Utrobicic⁹⁷, M. Vala¹¹⁴, J.W. Van Hoorne³⁶, M. van Leeuwen⁶⁴, P. Vande Vyvre³⁶, D. Varga¹⁴², A. Vargas², M. Vargyas¹²⁵, R. Varma⁴⁹, M. Vasileiou⁸⁴, A. Vasiliev⁸⁸, A. Vauthier⁷⁹, O. Vázquez Doce^{103,115}, V. Vechemin¹³⁷, A.M. Veen⁶⁴, E. Vercellin²⁸, S. Vergara Limón², L. Vermunt⁶⁴, R. Vernet⁸, R. Vértesi¹⁴², L. Vickovic³⁷, J. Viinikainen¹²⁵, Z. Vilakazi¹²⁸, O. Villalobos Baillie¹⁰⁸, A. Villatoro Tello², A. Vinogradov⁸⁸, T. Virgili³², V. Vislavicius^{89,81}, A. Vodopyanov⁷⁶, M.A. Völk¹⁰¹, K. Voloshin⁶⁵, S.A. Voloshin¹⁴⁰, G. Volpe³⁵, B. von Haller³⁶, I. Vorobyev^{115,103}, D. Voscek¹¹⁴, D. Vranic^{104,36}, J. Vrláková⁴⁰, B. Wagner²⁴, H. Wang⁶⁴, M. Wang⁷, Y. Watanabe¹³⁰, M. Weber¹¹¹, S.G. Weber¹⁰⁴, A. Wegrzynek³⁶, D.F. Weiser¹⁰², S.C. Wenzel³⁶, J.P. Wessels¹⁴¹, U. Westerhoff¹⁴¹, A.M. Whitehead¹²³, J. Wiechula⁷⁰, J. Wikne²³, G. Wilk⁸⁵, J. Wilkinson⁵⁴, G.A. Willems^{141,36}, M.C.S. Williams⁵⁴, E. Willsher¹⁰⁸, B. Windelband¹⁰², W.E. Witt¹²⁷, R. Xu⁷, S. Yalcin⁷⁸, K. Yamakawa⁴⁶, S. Yano⁴⁶, Z. Yin⁷, H. Yokoyama^{79,130}, I.-K. Yoo²⁰, J.H. Yoon⁶¹, V. Yurchenko³, V. Zaccolo⁵⁹, A. Zaman¹⁶, C. Zampolli³⁶, H.J.C. Zanolli¹¹⁹, N. Zardoshti¹⁰⁸, A. Zarochentsev¹³⁷, P. Závada⁶⁸, N. Zaviyalov¹⁰⁶, H. Zbroszczyk¹³⁹, M. Zhalov⁹⁶, X. Zhang⁷, Y. Zhang⁷, Z. Zhang^{7,131}, C. Zhao²³, V. Zherebchevskii¹³⁷, N. Zhigareva⁶⁵, D. Zhou⁷, Y. Zhou⁸⁹, Z. Zhou²⁴, H. Zhu⁷, J. Zhu⁷, Y. Zhu⁷, A. Zichichi^{29,11}, M.B. Zimmermann³⁶, G. Zinovjev³, J. Zmeskal¹¹¹, S. Zou⁷,

Affiliation notes

ⁱ Deceased

ⁱⁱ Dipartimento DET del Politecnico di Torino, Turin, Italy

ⁱⁱⁱ M.V. Lomonosov Moscow State University, D.V. Skobeltsyn Institute of Nuclear Physics, Moscow, Russia

^{iv} Department of Applied Physics, Aligarh Muslim University, Aligarh, India

^v Institute of Theoretical Physics, University of Wrocław, Poland

Collaboration Institutes

¹ A.I. Alikhanyan National Science Laboratory (Yerevan Physics Institute) Foundation, Yerevan, Armenia

² Benemérita Universidad Autónoma de Puebla, Puebla, Mexico

³ Bogolyubov Institute for Theoretical Physics, National Academy of Sciences of Ukraine, Kiev, Ukraine

⁴ Bose Institute, Department of Physics and Centre for Astroparticle Physics and Space Science (CAPSS), Kolkata, India

⁵ Budker Institute for Nuclear Physics, Novosibirsk, Russia

⁶ California Polytechnic State University, San Luis Obispo, California, United States

⁷ Central China Normal University, Wuhan, China

- 8 Centre de Calcul de l'IN2P3, Villeurbanne, Lyon, France
- 9 Centro de Aplicaciones Tecnológicas y Desarrollo Nuclear (CEADEN), Havana, Cuba
- 10 Centro de Investigación y de Estudios Avanzados (CINVESTAV), Mexico City and Mérida, Mexico
- 11 Centro Fermi - Museo Storico della Fisica e Centro Studi e Ricerche "Enrico Fermi", Rome, Italy
- 12 Chicago State University, Chicago, Illinois, United States
- 13 China Institute of Atomic Energy, Beijing, China
- 14 Chonbuk National University, Jeonju, Republic of Korea
- 15 Comenius University Bratislava, Faculty of Mathematics, Physics and Informatics, Bratislava, Slovakia
- 16 COMSATS Institute of Information Technology (CIIT), Islamabad, Pakistan
- 17 Creighton University, Omaha, Nebraska, United States
- 18 Department of Physics, Aligarh Muslim University, Aligarh, India
- 19 Department of Physics, Ohio State University, Columbus, Ohio, United States
- 20 Department of Physics, Pusan National University, Pusan, Republic of Korea
- 21 Department of Physics, Sejong University, Seoul, Republic of Korea
- 22 Department of Physics, University of California, Berkeley, California, United States
- 23 Department of Physics, University of Oslo, Oslo, Norway
- 24 Department of Physics and Technology, University of Bergen, Bergen, Norway
- 25 Dipartimento di Fisica dell'Università 'La Sapienza' and Sezione INFN, Rome, Italy
- 26 Dipartimento di Fisica dell'Università and Sezione INFN, Cagliari, Italy
- 27 Dipartimento di Fisica dell'Università and Sezione INFN, Trieste, Italy
- 28 Dipartimento di Fisica dell'Università and Sezione INFN, Turin, Italy
- 29 Dipartimento di Fisica e Astronomia dell'Università and Sezione INFN, Bologna, Italy
- 30 Dipartimento di Fisica e Astronomia dell'Università and Sezione INFN, Catania, Italy
- 31 Dipartimento di Fisica e Astronomia dell'Università and Sezione INFN, Padova, Italy
- 32 Dipartimento di Fisica 'E.R. Caianiello' dell'Università and Gruppo Collegato INFN, Salerno, Italy
- 33 Dipartimento DISAT del Politecnico and Sezione INFN, Turin, Italy
- 34 Dipartimento di Scienze e Innovazione Tecnologica dell'Università del Piemonte Orientale and INFN Sezione di Torino, Alessandria, Italy
- 35 Dipartimento Interateneo di Fisica 'M. Merlin' and Sezione INFN, Bari, Italy
- 36 European Organization for Nuclear Research (CERN), Geneva, Switzerland
- 37 Faculty of Electrical Engineering, Mechanical Engineering and Naval Architecture, University of Split, Split, Croatia
- 38 Faculty of Engineering and Science, Western Norway University of Applied Sciences, Bergen, Norway
- 39 Faculty of Nuclear Sciences and Physical Engineering, Czech Technical University in Prague, Prague, Czech Republic
- 40 Faculty of Science, P.J. Šafárik University, Košice, Slovakia
- 41 Frankfurt Institute for Advanced Studies, Johann Wolfgang Goethe-Universität Frankfurt, Frankfurt, Germany
- 42 Gangneung-Wonju National University, Gangneung, Republic of Korea
- 43 Gauhati University, Department of Physics, Guwahati, India
- 44 Helmholtz-Institut für Strahlen- und Kernphysik, Rheinische Friedrich-Wilhelms-Universität Bonn, Bonn, Germany
- 45 Helsinki Institute of Physics (HIP), Helsinki, Finland
- 46 Hiroshima University, Hiroshima, Japan
- 47 Hochschule Worms, Zentrum für Technologietransfer und Telekommunikation (ZTT), Worms, Germany
- 48 Horia Hulubei National Institute of Physics and Nuclear Engineering, Bucharest, Romania
- 49 Indian Institute of Technology Bombay (IIT), Mumbai, India
- 50 Indian Institute of Technology Indore, Indore, India
- 51 Indonesian Institute of Sciences, Jakarta, Indonesia
- 52 INFN, Laboratori Nazionali di Frascati, Frascati, Italy
- 53 INFN, Sezione di Bari, Bari, Italy
- 54 INFN, Sezione di Bologna, Bologna, Italy
- 55 INFN, Sezione di Cagliari, Cagliari, Italy
- 56 INFN, Sezione di Catania, Catania, Italy
- 57 INFN, Sezione di Padova, Padova, Italy
- 58 INFN, Sezione di Roma, Rome, Italy

- 59 INFN, Sezione di Torino, Turin, Italy
- 60 INFN, Sezione di Trieste, Trieste, Italy
- 61 Inha University, Incheon, Republic of Korea
- 62 Institut de Physique Nucléaire d'Orsay (IPNO), Institut National de Physique Nucléaire et de Physique des Particules (IN2P3/CNRS), Université de Paris-Sud, Université Paris-Saclay, Orsay, France
- 63 Institute for Nuclear Research, Academy of Sciences, Moscow, Russia
- 64 Institute for Subatomic Physics, Utrecht University/Nikhef, Utrecht, Netherlands
- 65 Institute for Theoretical and Experimental Physics, Moscow, Russia
- 66 Institute of Experimental Physics, Slovak Academy of Sciences, Košice, Slovakia
- 67 Institute of Physics, Bhubaneswar, India
- 68 Institute of Physics of the Czech Academy of Sciences, Prague, Czech Republic
- 69 Institute of Space Science (ISS), Bucharest, Romania
- 70 Institut für Kernphysik, Johann Wolfgang Goethe-Universität Frankfurt, Frankfurt, Germany
- 71 Instituto de Ciencias Nucleares, Universidad Nacional Autónoma de México, Mexico City, Mexico
- 72 Instituto de Física, Universidade Federal do Rio Grande do Sul (UFRGS), Porto Alegre, Brazil
- 73 Instituto de Física, Universidad Nacional Autónoma de México, Mexico City, Mexico
- 74 iThemba LABS, National Research Foundation, Somerset West, South Africa
- 75 Johann-Wolfgang-Goethe Universität Frankfurt Institut für Informatik, Fachbereich Informatik und Mathematik, Frankfurt, Germany
- 76 Joint Institute for Nuclear Research (JINR), Dubna, Russia
- 77 Korea Institute of Science and Technology Information, Daejeon, Republic of Korea
- 78 KTO Karatay University, Konya, Turkey
- 79 Laboratoire de Physique Subatomique et de Cosmologie, Université Grenoble-Alpes, CNRS-IN2P3, Grenoble, France
- 80 Lawrence Berkeley National Laboratory, Berkeley, California, United States
- 81 Lund University Department of Physics, Division of Particle Physics, Lund, Sweden
- 82 Nagasaki Institute of Applied Science, Nagasaki, Japan
- 83 Nara Women's University (NWU), Nara, Japan
- 84 National and Kapodistrian University of Athens, School of Science, Department of Physics, Athens, Greece
- 85 National Centre for Nuclear Research, Warsaw, Poland
- 86 National Institute of Science Education and Research, HBNI, Jatni, India
- 87 National Nuclear Research Center, Baku, Azerbaijan
- 88 National Research Centre Kurchatov Institute, Moscow, Russia
- 89 Niels Bohr Institute, University of Copenhagen, Copenhagen, Denmark
- 90 Nikhef, National institute for subatomic physics, Amsterdam, Netherlands
- 91 NRC Kurchatov Institute IHEP, Protvino, Russia
- 92 NRNU Moscow Engineering Physics Institute, Moscow, Russia
- 93 Nuclear Physics Group, STFC Daresbury Laboratory, Daresbury, United Kingdom
- 94 Nuclear Physics Institute of the Czech Academy of Sciences, Řež u Prahy, Czech Republic
- 95 Oak Ridge National Laboratory, Oak Ridge, Tennessee, United States
- 96 Petersburg Nuclear Physics Institute, Gatchina, Russia
- 97 Physics department, Faculty of science, University of Zagreb, Zagreb, Croatia
- 98 Physics Department, Panjab University, Chandigarh, India
- 99 Physics Department, University of Jammu, Jammu, India
- 100 Physics Department, University of Rajasthan, Jaipur, India
- 101 Physikalisches Institut, Eberhard-Karls-Universität Tübingen, Tübingen, Germany
- 102 Physikalisches Institut, Ruprecht-Karls-Universität Heidelberg, Heidelberg, Germany
- 103 Physik Department, Technische Universität München, Munich, Germany
- 104 Research Division and ExtreMe Matter Institute EMMI, GSI Helmholtzzentrum für Schwerionenforschung GmbH, Darmstadt, Germany
- 105 Rudjer Bošković Institute, Zagreb, Croatia
- 106 Russian Federal Nuclear Center (VNIIEF), Sarov, Russia
- 107 Saha Institute of Nuclear Physics, Kolkata, India
- 108 School of Physics and Astronomy, University of Birmingham, Birmingham, United Kingdom
- 109 Sección Física, Departamento de Ciencias, Pontificia Universidad Católica del Perú, Lima, Peru

- 110 Shanghai Institute of Applied Physics, Shanghai, China
- 111 Stefan Meyer Institut für Subatomare Physik (SMI), Vienna, Austria
- 112 SUBATECH, IMT Atlantique, Université de Nantes, CNRS-IN2P3, Nantes, France
- 113 Suranaree University of Technology, Nakhon Ratchasima, Thailand
- 114 Technical University of Košice, Košice, Slovakia
- 115 Technische Universität München, Excellence Cluster 'Universe', Munich, Germany
- 116 The Henryk Niewodniczanski Institute of Nuclear Physics, Polish Academy of Sciences, Cracow, Poland
- 117 The University of Texas at Austin, Austin, Texas, United States
- 118 Universidad Autónoma de Sinaloa, Culiacán, Mexico
- 119 Universidade de São Paulo (USP), São Paulo, Brazil
- 120 Universidade Estadual de Campinas (UNICAMP), Campinas, Brazil
- 121 Universidade Federal do ABC, Santo Andre, Brazil
- 122 University College of Southeast Norway, Tonsberg, Norway
- 123 University of Cape Town, Cape Town, South Africa
- 124 University of Houston, Houston, Texas, United States
- 125 University of Jyväskylä, Jyväskylä, Finland
- 126 University of Liverpool, Department of Physics Oliver Lodge Laboratory, Liverpool, United Kingdom
- 127 University of Tennessee, Knoxville, Tennessee, United States
- 128 University of the Witwatersrand, Johannesburg, South Africa
- 129 University of Tokyo, Tokyo, Japan
- 130 University of Tsukuba, Tsukuba, Japan
- 131 Université Clermont Auvergne, CNRS/IN2P3, LPC, Clermont-Ferrand, France
- 132 Université de Lyon, Université Lyon 1, CNRS/IN2P3, IPN-Lyon, Villeurbanne, Lyon, France
- 133 Université de Strasbourg, CNRS, IPHC UMR 7178, F-67000 Strasbourg, France, Strasbourg, France
- 134 Université Paris-Saclay Centre d'Études de Saclay (CEA), IRFU, Department de Physique Nucléaire (DPhN), Saclay, France
- 135 Università degli Studi di Pavia, Pavia, Italy
- 136 Università di Brescia, Brescia, Italy
- 137 V. Fock Institute for Physics, St. Petersburg State University, St. Petersburg, Russia
- 138 Variable Energy Cyclotron Centre, Kolkata, India
- 139 Warsaw University of Technology, Warsaw, Poland
- 140 Wayne State University, Detroit, Michigan, United States
- 141 Westfälische Wilhelms-Universität Münster, Institut für Kernphysik, Münster, Germany
- 142 Wigner Research Centre for Physics, Hungarian Academy of Sciences, Budapest, Hungary
- 143 Yale University, New Haven, Connecticut, United States
- 144 Yonsei University, Seoul, Republic of Korea